Cytokinetic furrowing in toroidal, binucleate and anucleate cells in *C. elegans* embryos

Jalal K. Baruni, Edwin M. Munro and George von Dassow*

Center for Cell Dynamics, Friday Harbor Laboratories, 620 University Road, Friday Harbor, WA 98250, USA and Department of Biology, University of Washington, Seattle, WA 98195, USA

*Author for correspondence (e-mail: dassow@u.washington.edu)

Accepted 24 October 2007
Journal of Cell Science 121, 306-316 Published by The Company of Biologists 2008
doi:10.1242/jcs.022897

Summary

Classical experimental studies on echinoderm zygotes concluded that the juxtaposition of two astral microtubule arrays localizes the stimulus for cytokinetic furrowing. However, recent experimental and genetic studies in *Caenorhabditis elegans*, *Drosophila* and mammalian cultured cells implicate microtubules of the central spindle, and regulatory proteins associated with this structure, suggesting that the essential conditions for furrow induction may differ from one animal cell to another. We used micromanipulation and laser microsurgery to create, in three ways, the juxtaposition of astral microtubules in *C. elegans* embryonic cells. In toroidal cells we observe that furrows initiate both where astral microtubule arrays are juxtaposed, and where the cortex most closely approaches the central spindle. We find that binucleate cells successfully furrow not only across the spindles, but also between unconnected spindle poles. Finally, we find that anucleate cells containing only a pair of centrosomes nevertheless attempt to cleave. Therefore, in *C. elegans* embryonic cells, as in echinoderms, juxtaposition of two asters suffices to induce furrowing, and neither the chromatin nor the physical structure of the central spindle are indispensable for furrow initiation. However, furrows that cross a central spindle are more likely to complete than those that do not.

Supplementary material available online at
http://jcs.biologists.org/cgi/content/full/121/3/306/DC1

Key words: *C. elegans*, Cell division, Central spindle, Cytokinesis

Introduction

Rappaport's creation of a toroidal sand dollar egg (Rappaport, 1961) yielded one of the most influential results in the history of research on animal cell cytokinesis (reviewed by Pollard, 2004). After perforation of the cell with a glass probe, confining the mitotic apparatus to one side of the torus, the cell mounted a cytokinetic furrow between the two spindle poles, creating a binucleate, U-shaped cell. At second cleavage each arm of the U contained one nucleus, which formed one mitotic apparatus. The cell mounted furrows not only across each spindle but also between them at the base of the U. This is interpreted to mean that juxtaposition of two spindle poles suffices to induce furrowing in the cortex. Because of the presumption that something associated with the spindle poles physically influences the cortex itself, attention has focused on the astral microtubule array emanating from each spindle pole. Subsequent experiments by Rappaport and others suggest that something about the asters promotes cortical contractility, that other constituents of the mitotic apparatus (such as chromosomes) have little influence on furrowing, and that the mitotic apparatus becomes dispensable once the stimulus has been transmitted. In particular, Hiramoto demonstrated furrowing in echinoderm eggs from which he had physically removed the nucleus (Hiramoto, 1971).

Several investigators have confirmed that adjacent spindle poles induce furrowing, either by repeating the perforation experiment in echinoderms (Shuster and Burgess, 2002) or by assessing furrow formation in binucleate cultured cells (e.g. Rieder et al., 1997; Sanger et al., 1998). However, in one of the few attempts at a direct analogy to Rappaport's perforation in cultured somatic cells, Cao and Wang (Cao and Wang, 1996) concluded that mammalian cells do not behave as Rappaport's experiments predict. They perforated flattened, mitotic cells with a microneedle, and found that astral microtubules densely penetrated the space beyond the perforation, where furrowing would normally occur, yet no furrow appeared beyond the perforation. Instead, the side of the perforation immediately adjacent to the central spindle became cytokinetically active. Cao and Wang concluded that in mammalian cells the central spindle is the principal agent of furrow induction. Wheatley and Wang (Wheatley and Wang, 1996) further concluded that midzone microtubules must be continually present to support furrowing between adjacent spindle poles.

Genetic studies in *Drosophila* and *C. elegans*, and RNAi studies in mammalian cells, show beyond doubt that proteins localized to the central spindle have an essential role at least in maintenance of the cytokinetic apparatus, and probably also in its induction (Bringmann and Hyman, 2005; D'Avino et al., 2006; Dechant and Glotzer, 2003; Jantsch-Plunger et al., 2000; Mishima et al., 2002; Nishimura and Yonemura, 2006; Somers and Saint, 2003; Yuce et al., 2005). The small GTPase RhoA has emerged as an essential physiological link between the geometry of the mitotic apparatus and cytokinetic furrow induction in diverse cells (Bement et al., 2005; Dean et al., 2005; Jantsch-Plunger et al., 2000; Yuce et al., 2005). Putative Rho regulators localize to the spindle midzone, and perhaps this population of regulators mediates local activation of Rho (D'Avino et al., 2006; Jantsch-Plunger et al., 2000; Mishima et al., 2002; Nishimura and Yonemura, 2006; Somers and Saint,

2003; Yuce et al., 2005). In addition to Rho regulators, other chromatin or central spindle components [such as Aurora B kinase (Murata-Hori and Wang, 2002)] appear at the furrow and in many cells are essential for furrow progression or completion (Kaitna et al., 2000; Severson et al., 2000). It is unknown, however, whether it is the same population of these factors that is found on the spindle which functions during furrowing.

Despite emerging evidence for a continuing role of the central spindle and chromosome passenger proteins throughout cytokinesis, experimental and genetic studies in *C. elegans* embryos continue to implicate centrosome position or astral microtubule geometry in furrow specification. Dechant and Glotzer (Dechant and Glotzer, 2003) showed that the central spindle only becomes essential for furrow *initiation* if the asters are closer than normal after anaphase, and concluded that the central spindle acts redundantly with a cue based on astral microtubule density. An elegant study by Bringmann and Hyman (Bringmann and Hyman, 2005) suggests that in *C. elegans* both asters and central spindle can separately induce furrowing, but the central spindle cue is both later-acting and dominant. Finally, Werner et al. (Werner et al., 2007) showed conclusively that two furrowing cues can be genetically or spatially separated in *C. elegans* zygotes. These experiments predict how the *C. elegans* embryo would behave in response to the same perturbations conducted in classical studies upon urchin eggs, and here we test those predictions directly.

We report our success conducting, in *C. elegans* zygotes and early embryonic blastomeres, the central experiments from the Rappaport and Hiramoto canon: perforation to create a toroidal cell, juxtaposition of asters unconnected by a spindle, and creation of anucleate cells. We find that *C. elegans* broadly follows the same rules deduced for echinoderm embryos: juxtaposition of two spindle poles can induce furrowing, and the nucleus and central spindle are, in Hiramoto's words, 'not indispensable for the formation of cleavage furrow' (Hiramoto, 1971). Yet we corroborate the findings of both Cao and Wang, and Bringmann and Hyman, in that, given a choice, the cell ratifies whichever furrow crosses a spindle midzone.

Results

Furrowing in toroidal *C. elegans* blastomeres

In Rappaport's seminal experiment, deformation of the mitotic cell into a torus segregates spatially any possible furrow-inducing cues emitted by the central spindle or chromatin from influences associated with the asters (Rappaport, 1961). To accomplish the analogous experiment in *C. elegans* embryos, we chemically removed the eggshell, then perforated cells one at a time (either the zygote or one of two cells) using a microneedle whose tip was fashioned into a spherical bead. The bead was slowly pushed through the cell until it contacted the coverslip, interposing a cylinder of cortex between the spindle and the equatorial cortex (Fig. 1A). The probe remained in place throughout the experiment. Perforated cells were very fragile, and were easily lysed by vibration transmitted through the probe. More than half our attempts suffered this fate.

Nevertheless, as long as they did not lyse, perforation disrupted surprisingly little about the behavior of cells. Perforated cells cleaved, and the time between anaphase onset and furrow initiation was nearly normal (median 141 seconds, n=6 perforated embryos, versus 112 seconds, n=9 controls). Perforated embryos expressing GFP-tubulin made a mitotic apparatus of normal structure including a central spindle that persisted after anaphase, and astral microtubules throughout the cell, including beyond the perforation toward what would have been the equatorial cortex (not shown). Furthermore, spindle orientation and displacement to the posterior in P0 (the zygote) proceeded normally: the position of the metaphase plate at anaphase onset was indistinguishable from normal (median 45% egg length, n=6 perforated embryos, versus 45% egg length, n=13 controls). This is perhaps surprising given how drastically perforation alters the geometry.

All P0 perforations described here were performed prior to the posterior displacement of the spindle during anaphase. Perforations of AB (the anterior cell of the two-cell embryo; the posterior cell is P1) were conducted in prophase or metaphase. We found it impossible to reposition the probe, once inserted, without lysing the cell, and therefore it was not always possible to position the bead directly beside the central spindle. We dubbed as 'misses' and scored separately all cases in which the

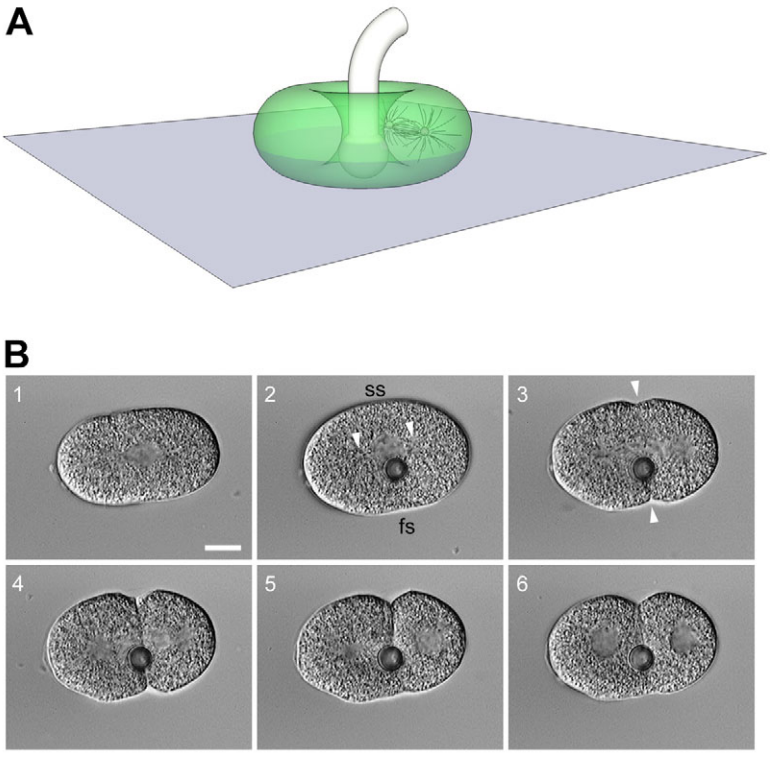

Fig. 1. Cytokinesis in toroidal *C. elegans* embryos. (A) Complete perforation interposes a cylinder of cell cortex between the mitotic apparatus and what would have been the equatorial cortex; no latitudinal connection exists between the cortex surrounding the mitotic apparatus and the cortex on the opposite side of the probe. (B) Frames from a DIC film of perforation and subsequent cytokinesis (supplementary material Movie 1). Frame 1 shows the dechorionated zygote at metaphase, still in its vitelline envelope. Anterior is to the left in all figures. Frame 2 is immediately following perforation with a probe ~5 μm in diameter. Arrowheads indicate spindle poles; ss, spindle side, fs, far side from the perforation. A furrow forms on both the far side and spindle side (frame 3); in this case, both furrows ingress deeply (frame 4), but the far-side furrow regresses (frame 5) shortly after nuclei reappear. The spindle-side furrow completes (frame 6), yielding a U-shaped, binucleate cell. Bar, 10 μm.

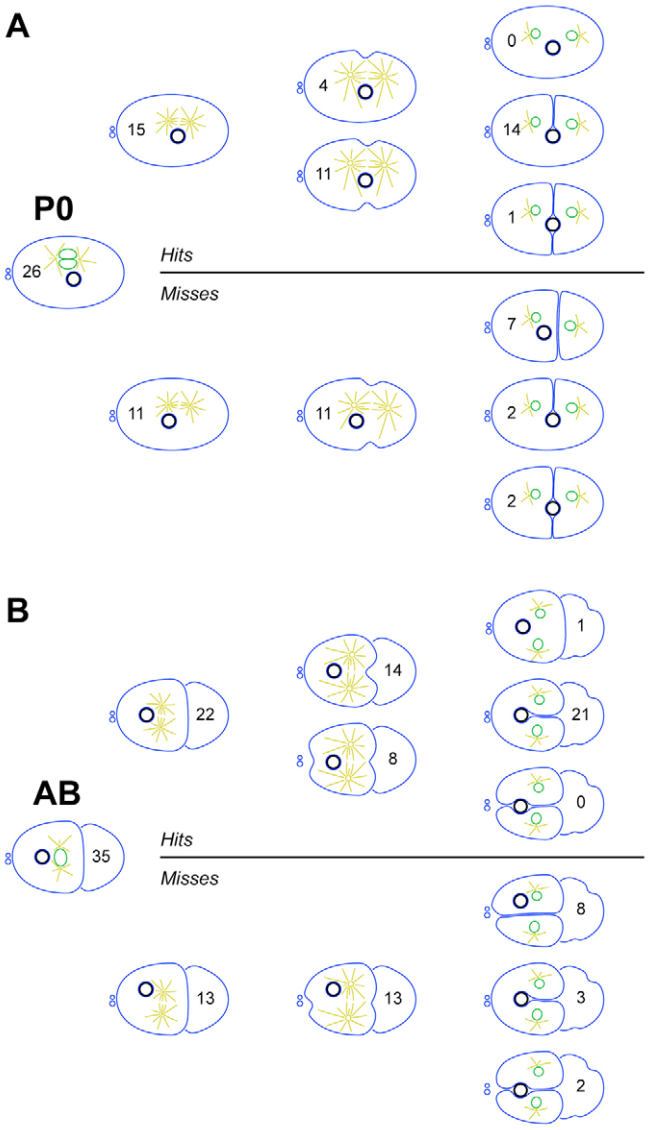

Fig. 2. Results from perforation of wild-type zygotes (P0) and the anterior cell (AB) of the two-cell embryo. Numbers shown include all cases, whether filmed with transmitted light or using NMY-2::GFP, in which perforation unambiguously preceded anaphase onset. (A) Most perforated P0 cells exhibit two overt furrows, but in the vast majority only the spindle-side furrow is stable. If the probe fails to intercept the space between the spindle midzone and the equator, then typically a furrow forms around the equator, seemingly ignoring the probe. In some cases the cortex surrounding the probe participates, and may yield a U-shaped binucleate cell, or cleavage may eliminate the probe from both cells. (B) In perforated AB, overt furrowing is less frequent on the far side of the probe (although the far side always exhibits myosin recruitment; see Fig. 3). As in P0, almost all AB in which the probe lies directly between the mitotic apparatus and the far-side cortex, successfully cleave only on the spindle side, yielding a binucleate U-shaped cell.

perforation was offset along the spindle axis such that the expected division plane did not intersect the perforation. In the majority of 'missed' cases, in both P0 and AB, cytokinesis proceeded to completion regardless of the perforation, yielding one normal and one toroidal daughter cell (tabulated results in Fig. 2). Occasionally, furrows that began in a plane not intersecting the perforation deflected towards the perforation as they ingressed. With approximately equal frequency, this resulted in either a U-shaped binucleate cell or stable divisions connecting both sides to the perforation (two uninucleate cells).

When the perforation was positioned between the central spindle and the equatorial cortex in P0, intersecting the expected cleavage plane, cleavage furrows usually (11/15) ingressed from both sides of the embryo (Fig. 1B; supplementary material Movie 1; tabulated results in Fig. 2A). In the remaining four cases, furrows only ingressed from the unobstructed side. Furrows that initiated on the far side, beyond the probe from the spindle, ingressed to varying extents before regressing; in only one unambiguous 'hit' did both furrows apparently complete. In the overwhelming majority, therefore, perforated zygotes cleaved to yield U-shaped, binucleate cells (14/15). Most successful perforations of AB also resulted in U-shaped cells (21/22). However, whereas overt furrows were usually apparent on both sides of perforated P0, most perforated AB exhibited overt furrowing only from the unobstructed side (14/22).

Myosin recruitment in toroidal cells

Furrowing is, ironically, a poor criterion for cytokinetic apparatus induction. First, the cell surface may be deformed passively, or by means other than cytokinetic apparatus function. Second, induction may occur, yet fail to achieve an overt furrow. Therefore, we also used recruitment of myosin, detected using NMY-2::GFP (Munro et al., 2004), as a more immediate readout of cytokinetic signaling. In wild-type perforated cells expressing NMY-2::GFP, we consistently observed that (1) myosin recruitment prefigures overt furrowing on both obstructed and unobstructed sides; (2) myosin is recruited prominently to the spindle side of the probe; and (3) myosin recruitment usually takes place on the far side equatorial cortex whether or not an overt furrow develops (Fig. 3).

At the time perforations were performed (late interphase to early metaphase), cortical myosin is either present in an anterior cap (in P0) or uniformly (in AB). In P0, the anterior cap disappears at metaphase, and the first manifestation of cytokinetic myosin recruitment is a population of broadly distributed blotches that persist and collect in the equatorial zone (Werner et al., 2007). This pattern was unaffected by perforation: myosin blotches appeared on both obstructed and unobstructed sides (Fig. 3A) in all nine successfully perforated, wild-type, GFP-myosin-expressing zygotes. They were not apparent on the cortex surrounding the probe. Myosin accumulation was often much weaker on the far side even when an overt furrow developed (Fig. 3A, typically as in frames 3-5; but see Fig. 5B frame 1).

In normal AB, myosin is enriched all over the cortex in prophase; the first sign of cytokinesis is the disappearance of cortical myosin from the cell poles, leaving a broad band which intensifies around the equator. This was evident on the obstructed side in nearly all toroidal, GFP-myosin-expressing AB cells (15/16), whether or not a furrow actually ingressed (Fig. 3B). In both P0 and AB, myosin also recruited very strongly to the spindle side of the cortex surrounding the probe. In wild-type cells, the spindle side of the probe acquired a noticeable myosin zone within 20 seconds after appearance of the equatorial band (all but one of 16 cases, scored as a 'miss' in Fig. 2). This accumulation appeared to connect to the equatorial zone on the unobstructed side, thus forming the complete furrow that successfully cleaved to yield a U-shaped cell. In wild-type cells we rarely observed a zone of myosin accumulation on the side of the perforation facing away from the spindle (2/16).

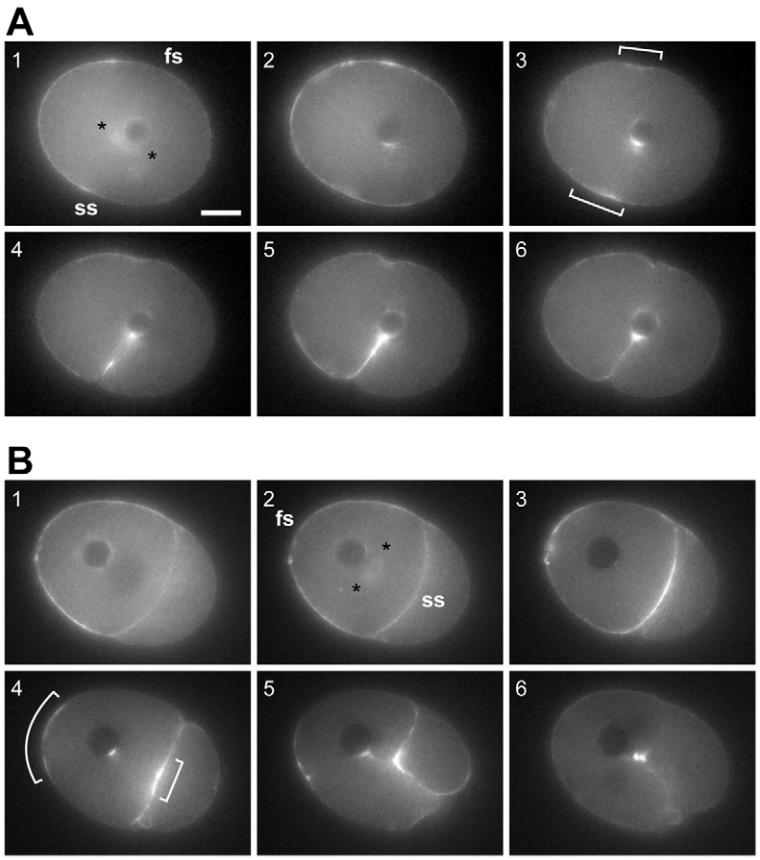

Fig. 3. Perforated cells consistently recruit myosin II to the far-side equatorial cortex. (A) Frames from a time-lapse sequence of a perforated zygote. In frame 1 asterisks indicate the approximate position of the spindle poles, inferred from the cloud of GFP-myosin that appears on the metaphase spindle. In both unmanipulated and perforated zygotes, the first phase of cytokinetic myosin recruitment is an array of blotches (frame 2), which appear broadly on the cell surface, then rapidly resolve into an equatorial band. Brackets in frame 3 mark the extent of the equatorial myosin zone on both the spindle side and far side. Often, as in this case, the far-side myosin zone is noticeably fainter than the spindle-side zone (although see Fig. 5B). Nevertheless this weak zone coincides with a shallow, persistent furrow (this embryo was scored for two furrows in Fig. 2A). The cortex around the probe recruits myosin intensely on the side facing the spindle. (B) Frames from a time-lapse sequence of a perforated AB. Frame 1 is before nuclear envelope breakdown; myosin is present everywhere on the cortex in AB, but not P1, before anaphase. Asterisks in frame 2 mark the approximate positions of spindle poles. During anaphase, myosin disappears from the polar cortex, but remains and brightens on both the spindle-side and far-side equatorial cortex (frame 3). The cortex between the probe and the spindle also develops an intense myosin zone (frame 4; brackets indicate the approximate extent of equatorial myosin zones) and, although myosin persists on the far side cortex, in this case furrowing occurs only on the spindle side (frame 5; this embryo was scored for one furrow in Fig. 2B). Shortly after nuclei reappear (dark spots, frame 6) myosin can no longer be detected on the far-side cortex. Bar, 10 μm; ss, spindle side; fs, far side from the perforation.

Role of the central spindle in toroidal cells

To explore the dependence of furrowing in perforated cells upon the central spindle, we perforated embryos depleted of either SPD-1 or ZEN-4 by feeding RNAi. SPD-1 is a midzone-specific microtubule bundling protein which is essential for the integrity of the central spindle, yet not for cytokinesis (Verbrugghe and White, 2004). SPD-1 depletion, therefore, tests the role of the physical structure. ZEN-4 is a kinesin that localizes to the central spindle midzone, and in contrast to SPD-1, is implicated in both the formation of the central spindle and localization of cytokinetic regulators (Mishima et al., 2002; Powers et al., 1998; Raich et al., 1998).

SPD-1-depleted embryos expressing GFP-tubulin form an apparently normal mitotic apparatus (Fig. 4A). We filmed five unperforated embryos, verifying that after 24 hours of RNAi feeding, the central spindle was absent. Chromosome separation proceeded and furrowing initiated; however, as the sister chromosomes pulled apart, little or no central spindle remained between them, and the spindle poles moved independently instead of behaving as ends of a connected whole. In unperforated SPD-1-depleted embryos cleavage was apparently normal, except for some apparent failures in EMS (the anterior daughter of P1 at the four-cell stage), as reported previously (Verbrugghe and White, 2004).

In all perforated SPD-1-depleted cells, NMY-2::GFP was recruited strongly to the spindle-side of the perforation following anaphase. Indeed, myosin accumulation on the cortex surrounding the probe began immediately after anaphase onset in many of the SPD-1-depleted cells, coincident with myosin accumulation on the peripheral equatorial cortex, whereas in wild-type perforated cells myosin began to accumulate on the probe only once the sister chromosomes were well separated. Meanwhile, cytokinetic zones that initiated on the obstructed equatorial side were more persistent, and more likely to ingress deeply, in SPD-1-depleted embryos (Fig. 4B,C). When the perforation was positioned between the central spindle and the equatorial cortex in ABs, overt myosin-enriched furrows ingressed from both sides of the cell in all seven cases; by contrast, although most perforated wild-type ABs recruit myosin to the far-side equatorial cortex, only about one in three develop an overt ingression (see Fig. 2). In most perforated, SPD-1-depleted ABs, the far-side furrow ingressed deeply before regressing; in two cases both furrows appeared to complete. In SPD-1-depleted P0, furrows ingressed from both sides in all three cases, and were deeper and more persistent than in wild-type cells. With difficulty we managed twice to perforate the EMS, the only cell that seems to have trouble cleaving in SPD-1-depleted embryos. To our surprise, both perforated EMS exhibited strong myosin recruitment to the spindle side of the probe, weak myosin recruitment to the equatorial cortex, and complete cleavage on *both* sides of the probe. Thus, even when we eliminate the central spindle, the cell nevertheless finds the patch of cortex nearest to the metaphase plate; both myosin recruitment and furrowing were more aggressive, not less, on both the probe cortex and the obstructed equator, in the absence of a detectable central spindle.

In ZEN-4-depleted but unperforated zygotes, furrows initiate, ingress deeply, and then regress (Mishima et al., 2002; Powers et al., 1998; Raich et al., 1998). Presumably because of the absence of a central spindle, during anaphase the spindle poles move rapidly apart, and, as in SPD-1-depleted cells, behave as if unconnected. Consistent with the interpretation that the perforation intercepts an inductive signal from the central spindle, in perforated ZEN-4-depleted embryos, we observed no *localized* myosin recruitment to the spindle-side of the perforation. However, in six out of eight cases, GFP-myosin accumulated around the probe in a rapidly oscillating,

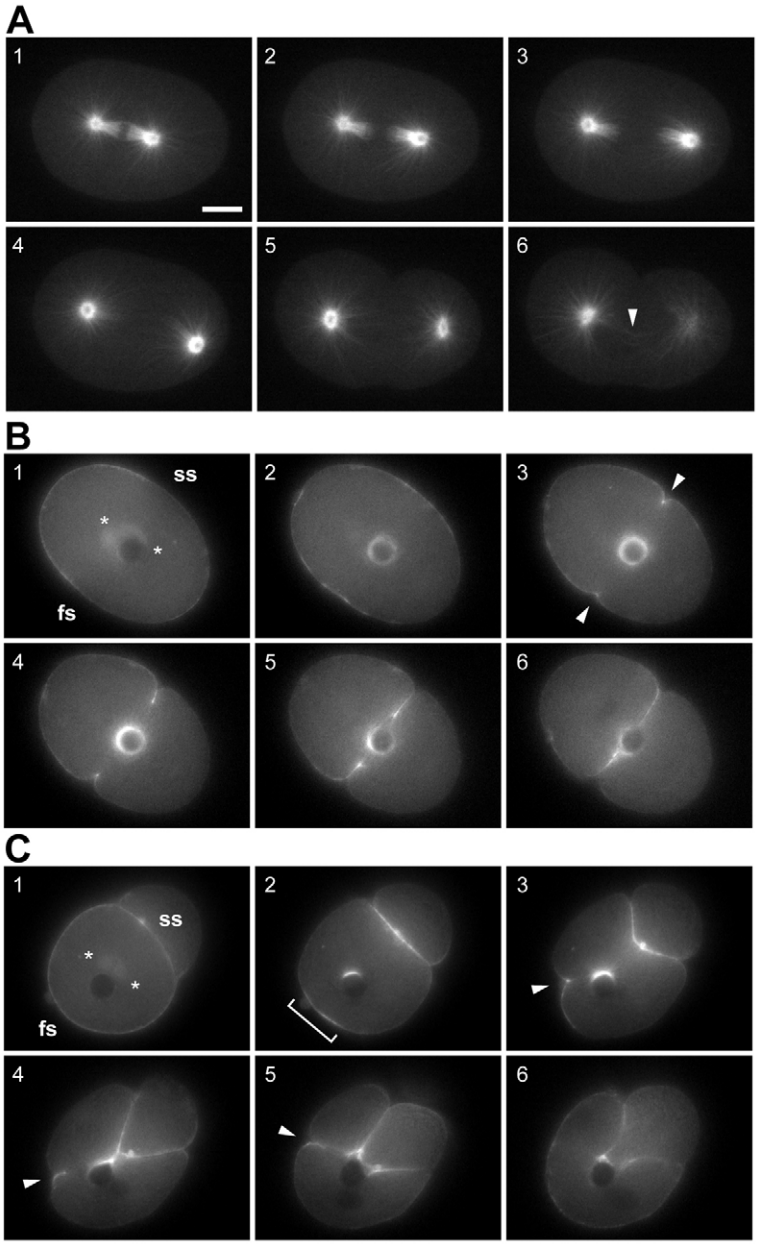

Fig. 4. SPD-1 depletion fails to abolish spindle-side furrowing, and makes far-side furrowing both deeper and more persistent. (A) Time-lapse sequence of the mitotic apparatus in a SPD-1-depleted zygote. The mitotic apparatus appears completely normal in metaphase (frame 1). When spindle poles move apart in anaphase, however, no microtubules remain between the separated chromosomes (frames 2 and 3). Kinetochore fibers break down, spindle poles swell, and furrowing initiates, as in wild-type embryos (frames 4 and 5). The only trace of the midzone microtubule array is a slender bundle of astral microtubules constricted by the cytokinetic furrow (frame 6, arrowhead). (B) Perforated SPD-1-depleted zygote. Asterisks in frame 1 mark the approximate position of spindle poles. The cortex around the probe recruits myosin uniformly instead of only on the side apposed to the spindle (frames 2-4). Furrows initiate both on the far side and spindle side of the perforation (frame 3, arrowheads). Both furrows ingress to completion (frames 4-6). (C) Perforated SPD-1-depleted AB. Asterisks mark approximate positions of spindle poles. Myosin recruitment takes place on the spindle side equatorial cortex, along the spindle side of the probe, and on the far side equatorial cortex (bracket in frame 2). Both far side and spindle side develop ingressions (frame 3; arrowhead in frames 3-5 marks the far-side furrow); at the time the spindle-side furrow completes (frame 4) the far side maintains a myosin-enriched furrow which ingresses deeply (frame 5), but ultimately regresses (frame 6). Bar, 10 μm; ss, spindle side; fs, far side from the perforation.

apparently contractile array (supplementary material Fig. S1). Both the initial GFP-myosin accumulation and the pulsing behavior were distributed uniformly about the perforation, displaying no detectable relationship to the original position of the mitotic apparatus. In addition, furrow ingression was attenuated in perforated ZEN-4-depleted embryos. In two cases, furrows ingressed deeply from both sides and then regressed, but in most (6/8), ingressions were either indistinguishable from cortical ruffling or entirely absent, despite myosin recruitment to the equatorial cortex. These results may indicate that without the centralspindlin protein complex, toroidal cells cannot easily maintain a continuous belt of contractile material around either equator.

Rappaport furrows in *C. elegans* embryos

Although in toroidal sand dollar zygotes, at the first division when the cell contains a single nucleus, a furrow appears only across the single spindle (Rappaport, 1961), we show above that toroidal *C. elegans* zygotes or blastomeres often develop furrows across both the central spindle and on the opposite side of the torus. Nevertheless, perforation of *C. elegans* zygotes or blastomeres usually yielded binucleate U-shaped cells because of the regression of the far-side furrow. We followed 14 such cells, resulting from perforation of zygotes, through the second division. Unfortunately, in many of these cells, the spindles orient orthogonally because of rotation of the posterior spindle, as they would in the unperforated two-cell stage. This geometry confounds our attempt to repeat Rappaport's experiment because it becomes impossible to tell whether any of the furrows are truly independent from a spindle midzone. In five cases, however, posterior spindle orientation failed, and the two spindles oriented such that unconnected asters were juxtaposed within a single focal plane. In all of these five, furrows were observed between the two asters unconnected by a central spindle, as in Rappaport's classic study (Fig. 5A,B).

The propensity of the mitotic spindle to re-orient in worm embryos likewise complicates this experiment in the U-shaped cell resulting from cleavage of perforated AB cells: in the next division spindles tend to align perpendicular to the focal plane. In two cases, spindles remained roughly aligned in the focal plane and a furrow formed between the two unconnected spindle poles. In either P0 or AB, Rappaport furrows usually failed to complete.

The low frequency with which we observed Rappaport furrows is apparently due not to the intrinsic nature of the cytokinetic mechanism – such furrows certainly occur – but rather to the confounding factor of spindle orientation. We attempted to eliminate this factor by perforating embryos depleted of PAR-2 by RNAi. In flattened but otherwise unharmed PAR-2-depleted embryos, spindles orient in parallel before second cleavage (Cheng et al., 1995). Tragically, in unflattened but perforated PAR-2-depleted embryos, one or the other spindle often escaped the focal plane because the spindle poles tended to adopt a tetrahedral configuration. Nevertheless, in about half (8/17) the spindles did lie parallel in the

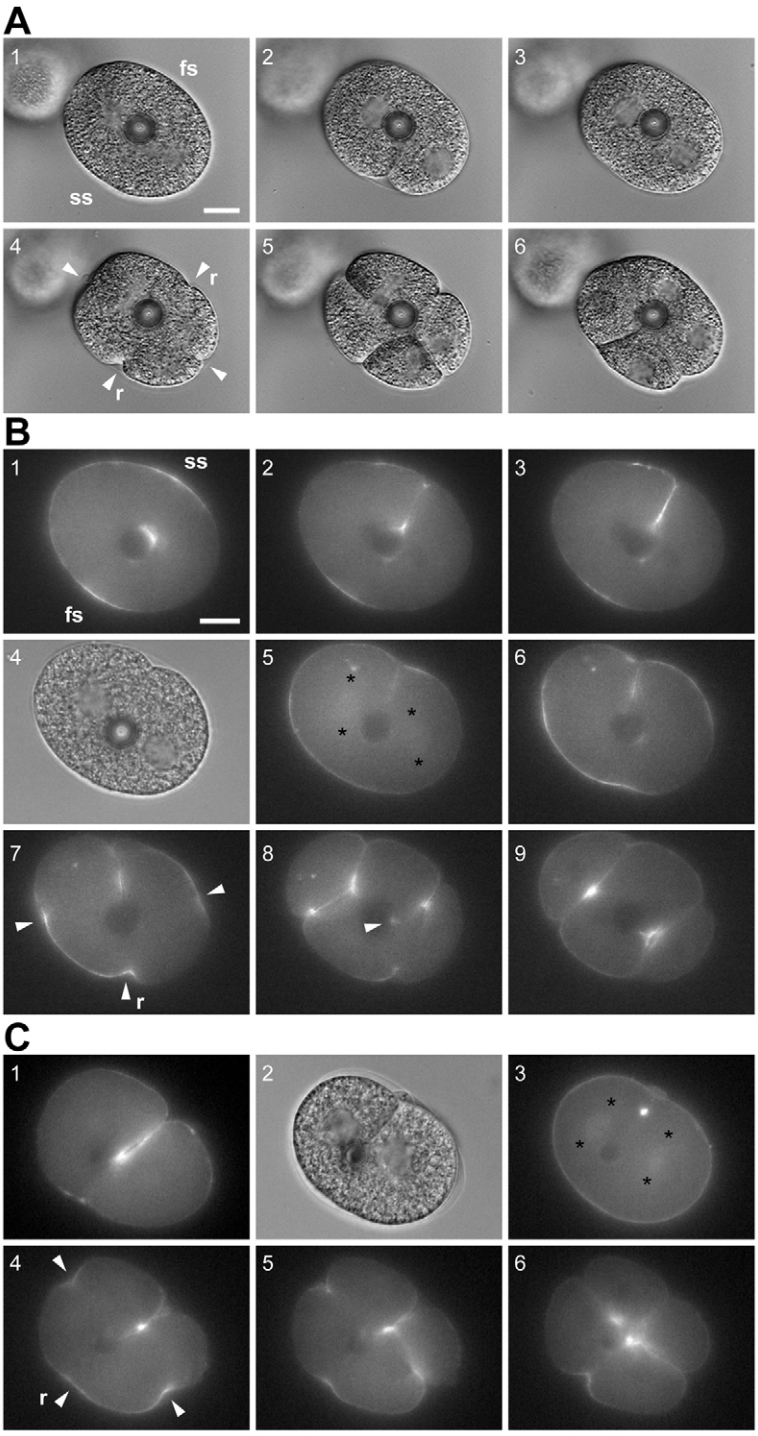

Fig. 5. Rappaport furrows in *C. elegans*. (A) A sequence of DIC images in which the spindle-side furrow failed to abscise (frame 3), yielding a toroidal binucleate cell. Since no cleavage scar exists to orient the posterior spindle, at second cleavage both spindles develop in parallel. Furrows form both across each spindle (arrowheads) and between the two pairs of spindle poles (arrowheads with 'r' for Rappaport furrow). Both the spindle-crossing and Rappaport furrows may ingress completely (frame 5) and remain stable, but Rappaport furrows are less likely to do so (one has regressed in frame 6; the other is stable). (B) A wild-type, perforated GFP-myosin-expressing zygote that exhibits furrowing between two unconnected spindle poles. Frames 1-3 show that this cell exhibited myosin recruitment to both the spindle-side and far-side cortex, and that as usual only the spindle-side furrow completed, yielding a U-shaped binucleate cell (frame 4). In this case the posterior spindle failed to align with the AP axis; asterisks in frame 5 indicate spindle poles. During cytokinesis three furrows initiate: around the anterior arm of the U, around the posterior arm, and between the two spindles (arrowheads in frame 7). The middle furrow represents an independent induction since the posterior arm of the U exhibits myosin recruitment to the probe cortex (arrowhead in frame 8). (C) A perforated, PAR-2-depleted zygote. Frame 1 shows that a furrow closed on the spindle side, yielding a binucleate U-shaped cell. Asterisks in frame 3 indicate the spindle poles. Furrowing begins across each spindle (frame 4), but myosin is also recruited between them, eventually resulting in a shallow but persistent furrow (frames 5 and 6). Bars, 10 μm; ss, spindle side; fs, far side from the perforation; r, Rappaport furrow.

focal plane as intended; in five, a furrow ingressed between the two spindles (Fig. 5C); in two other cases we observed cortical myosin recruitment between unconnected spindle poles but no furrow; in the last, we saw no sign of furrowing. We conclude that in *C. elegans*, juxtaposition of two asters can induce furrowing, but this induction is less reliable than when the furrow crosses a normal mitotic spindle.

Laser-induced cell fusion creates binucleate cells that divide one to four

Because of the scarcity of perforated cells in which the spindles aligned conveniently, we resorted to an alternate approach to create binucleate cells. We found that a very brief pulse with a highly focused UV laser, directed at the cell-cell interface, triggers fusion of two cells. With careful aim, a very small canal between two cells is immediately visible because of a rapid flow of cytoplasm. The remaining curtain of membrane between the two cells recedes over the next few minutes, yielding a binucleate cell. In a slight majority of cases (16/27) the two nuclei move together, in which case, upon nuclear envelope breakdown chromatin from each nucleus interacts with more than two spindle poles, creating a tangled, multipolar spindle. These cases are useless to us because, although they invariably divide from one to four cells, each daughter encompassing a centrosome and some nuclear material, the cleavage furrows generally cross a domain containing both chromatin and spindle fibers.

However, in the rest (11/27), the nuclei remained separate from fusion through mitosis, and two apparently unconnected spindles formed in the anterior and posterior halves of the binucleate cell (Fig. 6A,B, supplementary material Movie 2). In most such cases, the posterior spindle did not re-orient to lie along the anterior-posterior axis as it normally would, presumably because the spindle pole capture site at the cell-cell interface is lost. Because the embryos are flattened between the coverslip and an agar pad in this experiment, the anterior and posterior spindles are roughly parallel to one another. In all such cases, cytokinetic furrows formed not only across but also between the two spindles.

When we conducted this experiment in embryos expressing GFP-tubulin, we could detect no organized microtubules connecting the two spindles during the onset of furrowing (Fig. 6B). Furrowing often begins between the two spindles before it is apparent across them, and the furrow crossing the anterior spindle often seems, because of timing and direction, to be independent initially from the furrow crossing the posterior spindle. However, all furrows ultimately meet in the center, and in most cases

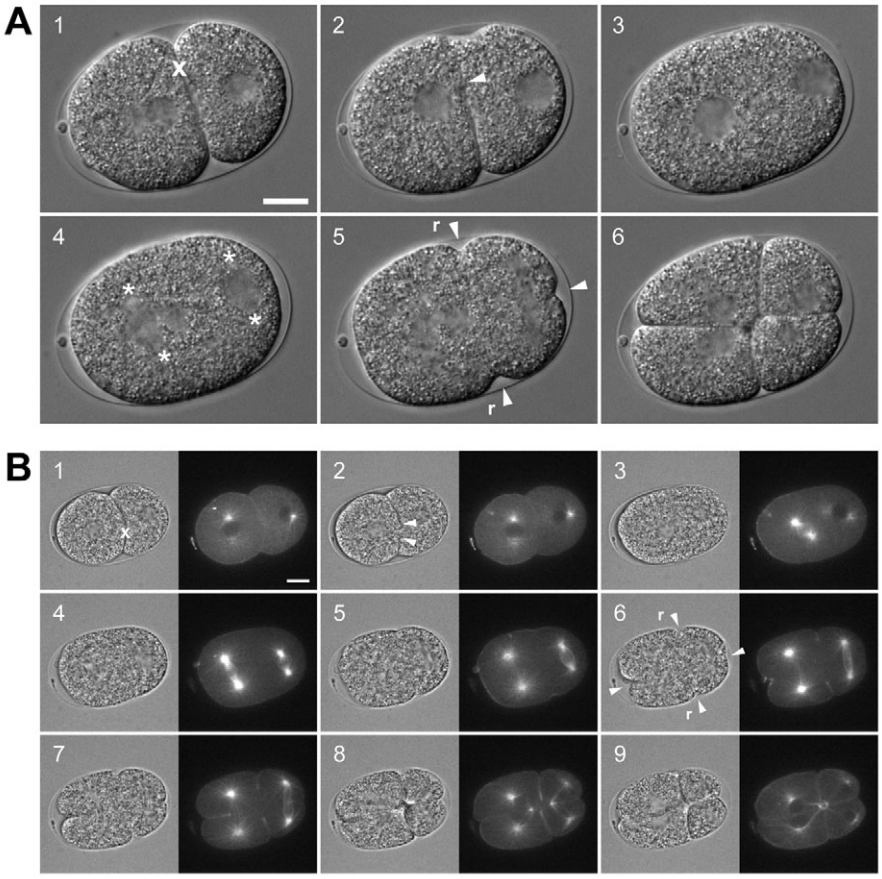

Fig. 6. Binucleate cells cleave from one to four. (A) A sequence of DIC images in which AB and P0 were fused in interphase. We fired several pulses from the UV laser at the cell-cell interface ('x' in frame 1). The hole rapidly widens as cytoplasm flows through; in frame 2 the arrowhead marks the edge of a curtain of withdrawing membrane. In this case, the nuclei remained separate during interphase (frame 3) and two independent spindles, oriented in parallel, developed at metaphase (frame 4). Furrows ingressed between each pair of spindle poles regardless of whether they shared a spindle (arrowheads in frame 5 indicate furrows; the fourth furrow, on the anterior, appeared later; 'r' for Rappaport indicates furrows that apparently bisect unconnected spindle poles). (B) Identical case to (A) but conducted in an embryo expressing both GFP-tubulin and GFP-myosin (supplementary material Movie 2). In frame 1 'x' indicates the fusion site; arrowheads in frame 2 indicate margins of the spreading hole. Nuclear envelope breakdown and spindle assembly occur sooner in the anterior nucleus (frame 3); two mitotic spindles form in parallel with no apparent connection between them (frames 4 and 5). Furrows initiate between each pair of spindle poles (arrowheads in frame 6). All furrows ingress deeply, meet near the center, and complete (frames 7-9), creating a four-cell embryo with an abnormal arrangement of cells. Bars, 10 μm.

complete abscission, completely partitioning the binucleate cell into four uninucleate cells. Some astral microtubules are drawn together by each furrow, whether it crosses a spindle or crosses just between two spindle poles. In this experiment furrows crossing a spindle were never observed to regress, but occasionally furrows between spindles failed to complete.

Laser-induced membrane fusion appears to cause no lasting damage to the cell cortex. In two instances the cells were fused during anaphase; the margins of the canal did not recede all the way, and the partly regressed margin was induced to recruit myosin and participate in cytokinetic furrowing within a minute (data not shown). This implies that fusion does not impair the competence of the cortex to assemble a contractile ring. Instead, one might worry that fusion would stimulate an actomyosin-dependent wound healing process as described in *Xenopus* oocytes (Mandato and Bement, 2001), which could, given the similarity of the wound array to the cytokinetic apparatus, deceive us into thinking that a cytokinetic furrow had been induced between the two spindles. We consider this unlikely because upon fusion during interphase and prophase the margins of the canal never exhibit myosin recruitment nor any inclination to draw themselves together.

Anucleate, centrosome-containing cells attempt cytokinesis

While attempting to repeat Bringmann and Hyman's spindle severing experiments (Bringmann and Hyman, 2005), we encountered a third situation in which to test the furrow-inducing capacity of the centrosomes. Bringmann and Hyman reported that upon severing the spindle pole from the rest of the spindle, cytokinetic furrowing first took place at the midpoint between the two spindle poles, then later initiated at a new site that bisected the central spindle. When we conducted the same experiment, we obtained this result in about 1 in 10 cases. More frequently, we found that the initial cytokinetic activity (either GFP-myosin recruitment or overt ingression/ruffling) occurred over a broader-than-normal domain. Cells in which one spindle pole was cut free of the mitotic apparatus usually initiated shallow ingressions in several nearby sites, but then furrowing soon became focused on a single area (supplementary material Fig. S2). Usually, this furrow succeeded in segregating the two sets of separated chromosomes.

Occasionally, however, the furrow failed to pass between the two sets of separated chromatin, especially if we cut the spindle before anaphase onset. Consequently, one daughter cell inherited both sets of chromatin, which either formed a single larger-than-normal nucleus, or formed two adjacent nuclei in the same cell. The other daughter inherited just a single spindle pole. Remarkably, all anucleate cells produced in this way (n=6) underwent several successive attempts at cytokinesis (Fig. 7A). To verify that the apparently anucleate cell lacked any chromatin, and to observe the behavior of centrosomes, we attempted these experiments in a strain expressing both GFP-gamma-tubulin and GFP-histone. In six cases we managed to create two-cell embryos in which either AB or P1 completely lacked detectable GFP-histone, but inherited a spindle pole. In all six, the single spindle pole in the anucleate daughter duplicated, whereupon the two daughter centrosomes separated from each other and adopted opposite positions in the deep cytoplasm. They swelled as they normally would prior to mitosis. Furrowing occurred between the two centrosomes. Most such furrows ingressed deeply, apparently cleaving the anucleate cell in two, but usually regressed at the time when one would expect abscission to take place (Fig. 7B,C; supplementary material

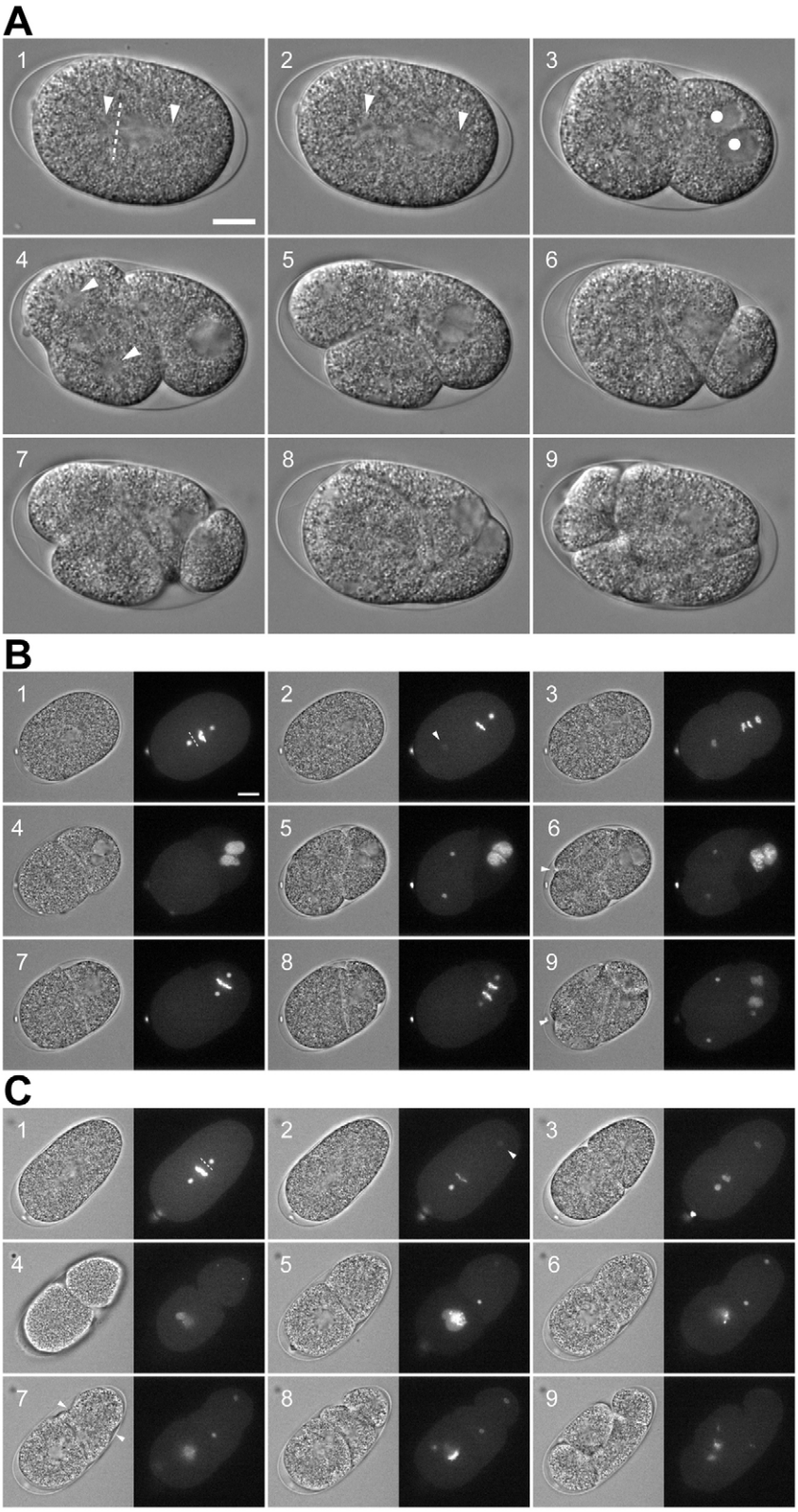

Fig. 7. Anucleate cells attempt cytokinesis. In each case one spindle pole was cut away from the rest of the mitotic apparatus (dashed line). (A) Frames from a DIC sequence in which the anterior spindle pole was severed. Arrowheads in frames 1 and 2 indicate the spindle poles immediately before and after severing. Cytokinesis partitions both daughter nuclei into the posterior cell (dots in frame 3); the anterior cell contains no visible nucleus, only a centrosome. After duplicating, centrosomes in the anucleate AB adopt opposite positions in the cell and a furrow develops between them (frame 4; arrowheads show centrosome position), ingresses deeply (frame 5), but eventually regresses (frame 6). P1 divides normally (frame 6). The anucleate AB attempts division repeatedly: frame 7 shows the second attempt (other furrows exist in other focal planes, as this cell attempts to divide into four) and frame 9 shows the third (at which point at least four, and probably eight, cytoplasmic domains are partitioned transiently by furrows). (B) The same experiment conducted in an embryo expressing both GFP-gamma tubulin and GFP-histone. Frames 1 and 2 show the metaphase spindle immediately before and after severing. Arrowhead marks the severed centrosome; although bleached by the laser, it recovers fluorescence rapidly (frame 3). After furrowing is completed, no chromatin is detected in AB. As in (A), the duplicated centrosomes adopt opposite positions (frame 5), and a furrow develops (arrowhead in frame 6). P1 enters metaphase as the furrow regresses in AB (frame 7), then divides normally, albeit late relative to AB (frame 8). In frame 9 AB attempts another division (see supplementary material Movie 3, which shows a similar case). (C) An embryo in which the posterior spindle pole was cut away at metaphase. Duplicated centrosomes appear as tiny dots (frame 4) which swell as the cell enters mitosis (frame 5), and, strikingly, adopt an alignment within the cell corresponding to the normal alignment of the spindle in P1; no chromatin is present between the centrosomes (frame 6). A deeply-ingressing furrow develops between the centrosomes in the anucleate P1 (frames 7-9; arrowheads in frame 7). This furrow apparently completed since it persisted at least 22 minutes. Bars, 10 μm.

Movie 3). We observed this outcome regardless of whether the anucleate daughter was AB or P1.

We found it astonishing how faithfully the isolated centrosomes in anucleate cells behaved as the spindle poles normally would. In anucleate AB cells, the two centrosomes aligned perpendicular to the focal plane as they normally would in a partially flattened embryo, and then the cell underwent a 90° rotation prior to cytokinesis; the centrosomes rotated with the cell contents into a medial focal plane as if they were connected by a rigid rod. In anucleate P1 cells, the centrosome pair underwent a 90° rotation, as the spindle normally would, such that one centrosome resided at the very posterior pole and the other about the site at which first cleavage completed (Fig. 7C). Despite this behavior, when we conducted the same experiment in embryos expressing GFP-tubulin, we detected no microtubules running between the two centrosomes (four of four cells that were successfully rendered anucleate), nor could we detect any such structure using DIC optics (data not shown).

Altogether we generated 16 anucleate cells (11 AB, 5 P1), every one of which attempted to cleave; in most (13/16) abscission failed. Anucleate cells underwent several successive attempts at cytokinesis (we observed as many as four attempts); centrosomes duplicated in each round, and multiple furrows formed, although it was not usually possible to verify, in a single focal plane, whether a furrow bisected every

pair. Successive cleavage attempts took place with approximately the same schedule as divisions would normally take place. Not so for their binucleate sisters; although some divided on schedule, others exhibited pronounced delays, occasionally with evident difficulty segregating chromosomes. This either reflects collateral damage to the chromatin from UV irradiation, or may imply that cells cannot easily manage an extra set of chromosomes.

Discussion

Bringmann and Hyman (Bringmann and Hyman, 2005) concluded that two signals, one dependent on aster position and the other based on proximity of the central spindle to the cortex, normally collude to direct furrowing in *C. elegans*. This corroborated the earlier work of Dechant and Glotzer (Dechant and Glotzer, 2003), who concluded that the furrow is normally positioned by the coincidence between a local minimum of astral microtubule density and the central spindle. Bringmann and Hyman (Bringmann and Hyman, 2005) showed that the first of these signals depends on Rho, the formin CYK-1 and myosin, whereas the central spindle cue depends on ZEN-4 and CYK-4, the centralspindlin complex, and that the central spindle signal normally supercedes the astral signal. The direct prediction is that if one conducted Rappaport's torus experiment in a worm egg, the furrowing stimulus would initially act on both obstructed and unobstructed sides (that is, the cortex-formerly-known-as-the-equator), then also on the spindle side of the cylinder of cortex surrounding the perforation. This we have now shown. Further, the spindle-side furrow should out-compete the far-side furrow. This also we have shown.

Yet our results do not accord in every way. First, we only rarely achieved the double furrow described by Bringmann and Hyman; we usually observed sloppy initial furrows that rapidly resolved into a single deep ingression that succeeded to partition sister chromosome sets. Having made well over a hundred attempts in various genetic backgrounds, in flattened and unflattened eggs, at various stages between metaphase and telophase, we remain unable to explain this discrepancy.

Second, Bringmann and Hyman found that in the absence of SPD-1, the aster-induced furrow proceeded to completion; no secondary furrow formed. However, since we find that SPD-1-depleted embryos still localize myosin to the perforation, usually on the spindle side, it seems overly facile to equate Bringmann and Hyman's secondary furrows with the activity we observe on the spindle side of the perforation. For the same reason we doubt that furrowing on the perforation could be credited to the astral signal. In other words, the cell appears to have all the normal positional information in the absence of SPD-1. That the perforation could uniformly recruit myosin is confirmed in ZEN-4-depleted embryos, which genuinely seem to lack positional information.

Bringmann and colleagues (Bringmann et al., 2007) conducted a screen for components of the 'astral pathway'. Assuming that *spd-1* mutants, lacking a central spindle, must depend solely on the astral mechanism, they sought genes required for zygote cytokinesis in a *spd-1* background but not wild-type cells, and concluded that the astral pathway depends on LET-99, heterotrimeric G-proteins, and the G-protein regulator GPR-1/2. These are implicated in spindle positioning (Rose and Kemphues, 1998; Tsou et al., 2002; Tsou et al., 2003), and LET-99 localizes to the cortex in a band prefiguring the furrow (Bringmann et al., 2007; Tsou et al., 2002). However, LET-99 localization cannot explain the 'astral pathway' in AB: previous reports show that LET-99 is uniformly distributed in AB (Tsou et al., 2002), but we show here that AB has the same propensity as zygotes to furrow between two asters.

Our results support the idea that the initial specification of the cytokinetic zone on the cell cortex is a relatively coarse spatial non-uniformity in the Rho- and Rho kinase-dependent recruitment of myosin II and unbranched actin filament assembly. A recent study suggests that astral microtubules locally inhibit myosin recruitment to bias furrow formation in just this way (Werner et al., 2007). Such a coarse pattern might self-amplify in *C. elegans*, because unlike some cells such as echinoderm zygotes and blastomeres, *C. elegans* blastomeres exhibit long-range actomyosin-driven cortical flow (Munro et al., 2004). The model of White and Borisy (White and Borisy, 1983), in which laterally mobile cortical tensile material flows and re-orients as it contracts, thus creating a self-amplifying anisotropy in the cell equator, may be a good hypothesis for furrow initiation in *C. elegans*.

Our results are further consistent with the idea that once furrowing initiates, progress depends on active maintenance by factors normally localized to the central spindle. Consider the striking similarity to earlier events during zygotic polarization: here too, a spatial non-uniformity in actomyosin recruitment causes cortical flow during an 'establishment phase', which gives way to a 'maintenance phase' in which a distinct mechanism sustains the anterior actomyosin cap (Cuenca et al., 2003; Munro et al., 2004). Cortical flow during polarization shares a physiological basis with cytokinetic furrowing: both depend on Rho, Rho kinase, Rho regulators LET-21 and CYK-4, myosin II, and actin assembly through CYK-1 and profilin (Jenkins et al., 2006; Motegi and Sugimoto, 2006; Schonegg and Hyman, 2006; Severson et al., 2002). The pseudo-cleavage furrow, lacking any obvious analogue to the central spindle, regresses similarly to cleavage furrows in embryos lacking ZEN-4 or CYK-4: after ingressing deeply, it loses actomyosin, discharges tension, and regresses.

What does the central spindle do to maintain furrowing to completion? Since many cytokinetic regulators localize to the spindle midzone, this structure seems like a signaling center (Jantsch-Plunger et al., 2000; Kaitna et al., 2000; Mishima et al., 2002). This hypothesis is incomplete, however, because SPD-1-depleted embryos clearly lack a central spindle after anaphase, yet clearly complete furrowing (Verbrugghe and White, 2004). Myosin recruitment near where the central spindle would have been is more rapid and aggressive without the central spindle, and furrows on the far side of the perforation are likewise more insistent in SPD-1-depleted embryos. Bringmann and Hyman (Bringmann and Hyman, 2005) also reported that 'aster-positioned' furrows proceeded to completion in embryos lacking SPD-1 or KLP-7, both of which eliminate the central spindle without otherwise impairing cytokinesis.

We therefore propose that the central spindle behaves as a sink for one or more regulators, present in limiting quantities, which help maintain active furrowing. Perhaps in normal cells the central spindle hoards the principal supply of this hypothetical furrow-maintaining factor; only furrows that approach the central spindle have sufficient access to this hoard to continue. Candidates for the hoard include ZEN-4 and CYK-4, and Aurora B kinase and other chromosomal passenger proteins. In SPD-1-depleted embryos, the cell lacks the physical framework to maintain the hoard, but not the furrow maintenance factor itself. Verbrugghe and White (Verbrugghe and White, 2007) showed that ZEN-4::GFP localizes

to the equatorial cortex as well as the central spindle, and embryos mutant for *spd-1* retain cortical equatorial localization of ZEN-4.

This might explain why SPD-1-depleted embryos seem to have all the positional information, but less selectivity about which furrow should persist, and why anucleate cells, also lacking a central spindle, typically proceed further with furrowing than would ZEN-4- or CYK-4-depleted cells: without a central spindle to hoard centralspindlin, perhaps more is available for deployment to the equatorial cortex. It may also explain why we find that, in *C. elegans*, Rappaport furrows in U-shaped cells often fail to complete, whereas furrows between unconnected spindles in binucleate cells usually *do* complete. In the former case, furrows crossing the spindles close at a different point than furrows between two asters; the latter never approach a central spindle. But in fused cells, all furrows draw together to the same point, thus all furrows eventually approach a spindle midzone. Similar fusion experiments in mammalian cells yield analogous results (Rieder et al., 1997).

In summary, we conducted direct analogues in worm embryos of four influential, and not all superficially compatible, micromanipulation experiments: Rappaport's torus (Rappaport, 1961), Cao and Wang's perforation (Cao and Wang, 1996), Rieder and colleagues' cell fusion (Rieder et al., 1997), and Hiramoto's enucleation (Hiramoto, 1971). All of their results hold simultaneously for *C. elegans*. Are mammalian cells and echinoderm embryos different? First, had Cao and Wang been able to detect the furrowing stimulus, rather than just overt furrowing, they might have detected the stimulus on the far side of the perforation. Second, the potency of the asters in sand dollar zygotes may have been slightly overstated in derivative accounts. There is no doubt about Rappaport's basic result. We have done it ourselves in echinoid eggs, as have others (Shuster and Burgess, 2002). However, sand dollar eggs exhibit varying success at accomplishing Rappaport furrows (G.v.D., unpublished). Some complete and apparently abscise. Some barely furrow at all. Some mount a furrow between the two asters which ingresses deeply, then recedes. The variable success of Rappaport furrows in sand dollar zygotes suggests that even in echinoderms, there is something special about furrows that encounter a central spindle.

Materials and Methods

Worm strains and culture

Nematodes were cultured as described previously (Brenner, 1974). All strains were derived from Bristol (N2) wild type. We used the following transgenic strains: JJ1473 [*nmy-2::gfp* (Nance et al., 2003)]; OD3 and OD4 (both *pie-1::gfp::tba-2*; generously provided by Paul Maddox and Arshad Desai, University of California, CA); and TH32 [*pie-1::gfp::tbg-1*; *pie-1::gfp::h2b* (Desai et al., 2003)].

RNA interference

RNA interference was performed by the feeding method (Timmons and Fire, 1998). The following feeding strains were used: *par-2* (Kamath et al., 2001), *spd-1* (Verbrugghe and White, 2004) and *zen-4* (Dechant and Glotzer, 2003). Worms were placed on feeding plates as L4 larvae and embryos were manipulated and examined after >24 hours of incubation at 25°C.

Perforations

To perforate embryos, we removed their eggshells using a technique modified from that of Park and Priess (Park and Priess, 2003). We immersed embryos for 90 seconds in two parts NaClO (available chlorine 10-13%; Sigma 425044), one part 10 M KOH and one part water. Bleached embryos were rinsed three times in 0.25 M Hepes pH 7.0, placed in minimal embryonic growth medium (Edgar, 1995), and observed unflattened. We did not remove the vitelline membrane, hence bleached embryos retained their typical ellipsoid shape. Unperforated embryos thus prepared cleaved normally and developed at least through gastrulation.

Perforation needles were pulled from glass capillaries with a Sutter P-97 puller and fashioned into smooth, spherical beads 5-10 μm in diameter using a Narishige MF-900 microforge. We performed perforations with a Narishige hanging joystick oil hydraulic micromanipulator by gingerly pushing the probe through the cell and directly against the coverslip. We verified that perforation was complete both by focusing at the surface and by further lowering the probe until it slid laterally along the coverslip.

Imaging

Perforated embryos were filmed either using DIC on a Nikon TE2000 inverted microscope with a 60× PlanFluor 1.25 NA objective and Hamamatsu C2400 CCD camera or using epifluorescence on a Nikon TE2000 with a 60× PlanApo 1.4 NA objective and Hamamatsu ORCA-ER camera controlled by MetaMorph software. Illumination was shuttered between exposures. Because perforated embryos were prone to lysis if the probe vibrated even slightly, all experiments were performed with minimal use of shutters or filter wheels. In other experiments we used a CARV spinning disk confocal imager mounted on the same microscope. Image processing and measurement was performed using MetaMorph or ImageJ. No convolution filters were applied; some images were corrected for photobleaching by linear adjustment of white and black points; DIC images in Figs 1 and 5 were gamma-corrected.

Laser-induced membrane fusion and spindle severing

We used a Photonic Instruments' MicroPoint laser operating at 365 nm, 10-20 Hz, 50% attenuation, connected to a Nikon TE2000 inverted microscope. The laser was fired only long enough to achieve either flow of cytoplasm from one cell to another, or rapid separation of one pole from the mitotic apparatus. Experiments involving UV used a 60× PlanFluor 1.25 NA objective. To fuse membranes required only a few pulses, whereas to sever the spindle required panning back and forth, typically for 2-4 seconds, across the region to be cut. We made cuts immediately adjacent to, not overlapping, the pole itself. In our hands, severing the spindle requires enough irradiation to noticeably photobleach nearby cytoplasm.

We gratefully acknowledge Monica Castellanos' participation in initial stages of this work. We thank Karen Oegema, Jim Priess, Michael Glotzer and Koen Verbrugghe for worm and feeding strains, William Bement and Victoria Foe for reading the manuscript, and Chris Schoff and Garry Odell for helpful discussions. Some nematode strains were provided by the *Caenorhabditis* Genetics Center, which is funded by the NIH National Center for Research Resources (NCRR). This work was funded by NIH grant GM066050-02 to G.M.O.

References

Bement, W. M., Benink, H. A. and von Dassow, G. (2005). A microtubule-dependent zone of active RhoA during cleavage plane specification. *J. Cell Biol.* **170**, 91-101.

Brenner, S. (1974). The genetics of Caenorhabditis elegans. *Genetics* **77**, 71-94.

Bringmann, H. and Hyman, A. A. (2005). A cytokinesis furrow is positioned by two consecutive signals. *Nature* **436**, 731-734.

Bringmann, H., Cowan, C. R., Kong, J. and Hyman, A. A. (2007). LET-99, GOA-1/GPA-16, and GPR-1/2 are required for aster-positioned cytokinesis. *Curr. Biol.* **17**, 185-191.

Cao, L. G. and Wang, Y. L. (1996). Signals from the spindle midzone are required for the stimulation of cytokinesis in cultured epithelial cells. *Mol. Biol. Cell* **7**, 225-232.

Cheng, N. N., Kirby, C. M. and Kemphues, K. J. (1995). Control of cleavage spindle orientation in Caenorhabditis elegans: the role of the genes par-2 and par-3. *Genetics* **139**, 549-559.

Cuenca, A. A., Schetter, A., Aceto, D., Kemphues, K. and Seydoux, G. (2003). Polarization of the C. elegans zygote proceeds via distinct establishment and maintenance phases. *Development* **130**, 1255-1265.

D'Avino, P. P., Savoian, M. S., Capalbo, L. and Glover, D. M. (2006). RacGAP50C is sufficient to signal cleavage furrow formation during cytokinesis. *J. Cell Sci.* **119**, 4402-4408.

Dean, S. O., Rogers, S. L., Stuurman, N., Vale, R. D. and Spudich, J. A. (2005). Distinct pathways control recruitment and maintenance of myosin II at the cleavage furrow during cytokinesis. *Proc. Natl. Acad. Sci. USA* **102**, 13473-13478.

Dechant, R. and Glotzer, M. (2003). Centrosome separation and central spindle assembly act in redundant pathways that regulate microtubule density and trigger cleavage furrow formation. *Dev. Cell* **4**, 333-344.

Desai, A., Rybina, S., Muller-Reichert, T., Shevchenko, A., Shevchenko, A., Hyman, A. and Oegema, K. (2003). KNL-1 directs assembly of the microtubule-binding interface of the kinetochore in C. elegans. *Genes Dev.* **17**, 2421-2435.

Edgar, L. G. (1995). Blastomere culture and analysis. *Methods Cell Biol.* **48**, 303-321.

Hiramoto, Y. (1971). Analysis of cleavage stimulus by means of micromanipulation of sea urchin eggs. *Exp. Cell Res.* **68**, 291-298.

Jantsch-Plunger, V., Gonczy, P., Romano, A., Schnabel, H., Hamill, D., Schnabel, R., Hyman, A. A. and Glotzer, M. (2000). CYK-4: A Rho family gtpase activating protein (GAP) required for central spindle formation and cytokinesis. *J. Cell Biol.* **149**, 1391-1404.

Jenkins, N., Saam, J. R. and Mango, S. E. (2006). CYK-4/GAP provides a localized cue to initiate anteroposterior polarity upon fertilization. *Science* **313**, 1298-1301.

Kaitna, S., Mendoza, M., Jantsch-Plunger, V. and Glotzer, M. (2000). Incenp and an aurora-like kinase form a complex essential for chromosome segregation and efficient completion of cytokinesis. *Curr. Biol.* **10**, 1172-1181.

Kamath, R. S., Martinez-Campos, M., Zipperlen, P., Fraser, A. G. and Ahringer, J. (2001). Effectiveness of specific RNA-mediated interference through ingested double-stranded RNA in Caenorhabditis elegans. *Genome Biol*. **2**, RESEARCH0002.

Mandato, C. A. and Bement, W. M. (2001). Contraction and polymerization cooperate to assemble and close actomyosin rings around Xenopus oocyte wounds. *J. Cell Biol*. **154**, 785-797.

Mishima, M., Kaitna, S. and Glotzer, M. (2002). Central spindle assembly and cytokinesis require a kinesin-like protein/RhoGAP complex with microtubule bundling activity. *Dev. Cell* **2**, 41-54.

Motegi, F. and Sugimoto, A. (2006). Sequential functioning of the ECT-2 RhoGEF, RHO-1 and CDC-42 establishes cell polarity in Caenorhabditis elegans embryos. *Nat. Cell Biol*. **8**, 978-985.

Munro, E., Nance, J. and Priess, J. R. (2004). Cortical flows powered by asymmetrical contraction transport PAR proteins to establish and maintain anterior-posterior polarity in the early C. elegans embryo. *Dev. Cell* **7**, 413-424.

Murata-Hori, M. and Wang, Y. L. (2002). Both midzone and astral microtubules are involved in the delivery of cytokinesis signals: insights from the mobility of aurora B. *J. Cell Biol*. **159**, 45-53.

Nance, J., Munro, E. M. and Priess, J. R. (2003). C. elegans PAR-3 and PAR-6 are required for apicobasal asymmetries associated with cell adhesion and gastrulation. *Development* **130**, 5339-5350.

Nishimura, Y. and Yonemura, S. (2006). Centralspindlin regulates ECT2 and RhoA accumulation at the equatorial cortex during cytokinesis. *J. Cell Sci*. **119**, 104-114.

Park, F. D. and Priess, J. R. (2003). Establishment of POP-1 asymmetry in early C. elegans embryos. *Development* **130**, 3547-3556.

Pollard, T. D. (2004). Ray Rappaport chronology: twenty-five years of seminal papers on cytokinesis in the Journal of Experimental Zoology. *J. Exp. Zoolog. Part A Comp. Exp. Biol*. **301**, 9-14.

Powers, J., Bossinger, O., Rose, D., Strome, S. and Saxton, W. (1998). A nematode kinesin required for cleavage furrow advancement. *Curr. Biol*. **8**, 1133-1136.

Raich, W. B., Moran, A. N., Rothman, J. H. and Hardin, J. (1998). Cytokinesis and midzone microtubule organization in Caenorhabditis elegans require the kinesin-like protein ZEN-4. *Mol. Biol. Cell* **9**, 2037-2049.

Rappaport, R. (1961). Experiments concerning the cleavage stimulus in sand dollar eggs. *J. Exp. Zool*. **148**, 81-89.

Rieder, C. L., Khodjakov, A., Paliulis, L. V., Fortier, T. M., Cole, R. W. and Sluder, G. (1997). Mitosis in vertebrate somatic cells with two spindles: implications for the metaphase/anaphase transition checkpoint and cleavage. *Proc. Natl. Acad. Sci. USA* **94**, 5107-5112.

Rose, L. S. and Kemphues, K. (1998). The let-99 gene is required for proper spindle orientation during cleavage of the C. elegans embryo. *Development* **125**, 1337-1346.

Sanger, J. M., Dome, J. S. and Sanger, J. W. (1998). Unusual cleavage furrows in vertebrate tissue culture cells: insights into the mechanisms of cytokinesis. *Cell Motil. Cytoskeleton* **39**, 95-106.

Schonegg, S. and Hyman, A. A. (2006). CDC-42 and RHO-1 coordinate acto-myosin contractility and PAR protein localization during polarity establishment in C. elegans embryos. *Development* **133**, 3507-3516.

Severson, A. F., Hamill, D. R., Carter, J. C., Schumacher, J. and Bowerman, B. (2000). The aurora-related kinase AIR-2 recruits ZEN-4/CeMKLP1 to the mitotic spindle at metaphase and is required for cytokinesis. *Curr. Biol*. **10**, 1162-1171.

Severson, A. F., Baillie, D. L. and Bowerman, B. (2002). A Formin Homology protein and a profilin are required for cytokinesis and Arp2/3-independent assembly of cortical microfilaments in C. elegans. *Curr. Biol*. **12**, 2066-2075.

Shuster, C. B. and Burgess, D. R. (2002). Transitions regulating the timing of cytokinesis in embryonic cells. *Curr. Biol*. **12**, 854-858.

Somers, W. G. and Saint, R. (2003). A RhoGEF and Rho family GTPase-activating protein complex links the contractile ring to cortical microtubules at the onset of cytokinesis. *Dev. Cell* **4**, 29-39.

Timmons, L. and Fire, A. (1998). Specific interference by ingested dsRNA. *Nature* **395**, 854.

Tsou, M. F., Hayashi, A., DeBella, L. R., McGrath, G. and Rose, L. S. (2002). LET-99 determines spindle position and is asymmetrically enriched in response to PAR polarity cues in C. elegans embryos. *Development* **129**, 4469-4481.

Tsou, M. F., Hayashi, A. and Rose, L. S. (2003). LET-99 opposes Galpha/GPR signaling to generate asymmetry for spindle positioning in response to PAR and MES-1/SRC-1 signaling. *Development* **130**, 5717-5730.

Verbrugghe, K. J. and White, J. G. (2004). SPD-1 is required for the formation of the spindle midzone but is not essential for the completion of cytokinesis in C. elegans embryos. *Curr. Biol*. **14**, 1755-1760.

Verbrugghe, K. J. and White, J. G. (2007). Cortical centralspindlin and G{alpha} have parallel roles in furrow initiation in early C. elegans embryos. *J. Cell Sci*. **120**, 1772-1778.

Werner, M., Munro, E. and Glotzer, M. (2007). Astral signals spatially bias cortical myosin recruitment to break symmetry and promote cytokinesis. *Curr. Biol*. **17**, 1286-1297.

Wheatley, S. P. and Wang, Y. (1996). Midzone microtubule bundles are continuously required for cytokinesis in cultured epithelial cells. *J. Cell Biol*. **135**, 981-989.

White, J. G. and Borisy, G. G. (1983). On the mechanisms of cytokinesis in animal cells. *J. Theor. Biol*. **101**, 289-316.

Yuce, O., Piekny, A. and Glotzer, M. (2005). An ECT2-centralspindlin complex regulates the localization and function of RhoA. *J. Cell Biol*. **170**, 571-582.